FEBS Letters 397 (1996) 30–34 FEBS 17733

Topographical structure of membrane-bound *Escherichia coli* F_1F_0 ATP synthase in aqueous buffer

Seema Singh[a], Paola Turina[b], Carlos J. Bustamante[c], David J. Keller[a,*], Roderick Capaldi[b]

[a]*Department of Chemistry, University of New Mexico, Albuquerque, NM 87131, USA*
[b]*Institute of Molecular Biology, University of Oregon, Eugene, OR 97403-1229, USA*
[c]*Institute of Molecular Biology, Howard Hughes Medical Institute, University of Oregon, Eugene, OR 97403-1229, USA*

Received 11 September 1996

Abstract Scanning force microscope images of membrane-bound *Escherichia coli* ATP synthase F_0 complexes have been obtained in aqueous solution. The images show a consistent set of internal features: a ring structure which surrounds a central dimple and contains an asymmetric lateral mass. Images of trypsin-treated F_0 complexes, which have lost part of their b subunits, show a reduced asymmetric mass, while images of c-subunit oligomers, which lack both the a and b subunits, show a ring and dimple but do not have an asymmetric mass. These results support models in which the F_0 complex contains a ring of 9–12 c subunits with the b subunits located outside this ring, and show that scanning force microscopy is able to provide structural information on membrane proteins of molecular mass less than 200 000 Da.

Key words: ATP synthase; Scanning force microscopy; Atomic force microscopy; Tapping mode; Membrane protein

1. Introduction

F_1F_0 ATP synthases are large, multisubunit protein complexes found in the plasma membrane of bacteria, the mitochondrial inner membrane of animals and plants, and the chloroplast thylakoid membrane of plants, where they synthesize ATP from stored electrochemical energy in the form of a transmembrane proton gradient. The proton gradient is generated by electron transport chains associated with either oxidative phosphorylation or photosynthesis, and the F_1F_0 ATP synthases are the main source of ATP in all aerobic and photosynthetic organisms. Structurally, they are composed of two distinct parts: the F_0 sector, which is membrane integrated, and the F_1 sector which is normally joined to F_0 by a narrow stalk 40–45 Å in length [1–4]. The F_1 sector in all organisms is composed of five different subunits, α, β, γ, δ, and ε in the molar ratio 3:3:1:1:1, with catalytic sites located in each of the three β subunits. The recent high-resolution crystal structure of mitochondrial F_1 has provided detailed information on the α, β, and a major part of the γ subunit [5]. It shows the three α and three β subunits arranged in a hexagon with a long cylindrical hollow through the center. The γ subunit runs the length of this hollow and extends from one end to form part of the stalk. More recently, the structure of the ε subunit of ECF_1 (the *Escherichia coli* F_1) has been determined by NMR [6]. This subunit interacts with other F_1 subunits and also the c subunits of the F_0 sector and is, therefore, also a part of the stalk region.

The F_0 sector is much less characterized than the F_1 part. In its simplest form, as in *E. coli*, the F_0 sector contains only three different subunits, a, b, and c, in the stoichiometry 1:2:9–12 [3]. Chloroplast F_0 contains four types of subunits which appear to be similar to the *E. coli* subunits with an extra variant of subunit b [7]. In mitochondria, the F_0 sector has a core complex that seems to be similar to the *E. coli* F_0, but contains 5–8 additional subunits which probably play a regulatory role [8]. *E. coli* F_0 (ECF_0) is therefore a relatively simple model for the F_0s of many organisms.

The key function of F_0 is to act as a channel through which protons pass from high concentration on one side of the membrane to low concentration on the other. In ATP synthesis the energy provided by this proton translocation is transferred to the catalytic sites of the F_1 sector, through the stalk, over a distance of at least 90 Å. The mechanism of this energy transduction is an open question which is unlikely to be fully answered until the structure of F_0 is better known. To date, attempts to obtain either two-dimensional crystals for electron diffraction or three-dimensional crystals for X-ray diffraction have failed, and even the gross arrangement of the a, b, and c subunits within ECF_0 is not well defined, although several different models have been proposed [9,10].

To address this problem, scanning force microscopy (SFM) has been used to image *E. coli* F_0 in membrane bilayers. Recently, SFM has begun to emerge as a general method in structural biology. Several membrane proteins have been imaged successfully in two-dimensional crystals [11–13], and show the same features as have been identified by electron microscopy. Attempts to use SFM on membrane proteins that do not form ordered arrays are limited, but there are two recent reports: an analysis of the 124 MDa nuclear pore of *Xenopus laevis* [14], and a preliminary study of cholera toxin B-oligomers bound to model membranes [15]. In the present work, we show that it is possible to obtain SFM images of *E. coli* F_0 with sufficient resolution to reveal internal structural details and distinguish among competing models of the subunit arrangement of ECF_0.

2. Materials and methods

2.1. Sample preparation

ECF_1F_0 was prepared from the overproducing strain AN1460 as described by Foster et al. [16] and modified by Aggeler et al. [17]. Reverse-phase liposomes were prepared according to Szoka and Papahadjopoulos [18] in 20 mM glycylglycine, 20 mM succinic acid, 20 mM NaCl, pH 8.0 (buffer A). After ether evaporation, the suspension of vesicles (16 mg/ml egg phosphatidylcholine (egg PC) and 0.8 mg/ml egg phosphatidic acid) was filtered through polycarbonate membranes (Nucleopore) with 0.4 and 0.2 μm pore diameter in consecutive steps, yielding liposomes of approx. 150 nm. ECF_1F_0 was reconstituted into these preformed liposomes as described by Richard et al. [19] by mixing the liposome suspension with purified enzyme and Triton X-100 followed by slow removal of the detergent with BioBeads. The

*Corresponding author. Fax: (1) (505) 277-2609.

PII S0014-5793(96)01127-1

concentration of ECF_1F_0 was chosen so that the average number of protein complexes per vesicle was between 10 and 15. For such low enzyme concentration, this procedure has been shown to yield a uniform distribution of protein per vesicle and a uniform outwards orientation of F_1F_0 complexes. In all cases except the real-time stripping experiments, the F_0 sector was exposed for imaging by removing ('stripping') the F_1 sector as in Lötscher et al. [20]: Vesicle suspensions of ECF_1F_0 were pelleted (1 h at 285 000 × *g*) and resuspended in stripping buffer (0.5 mM HEPES, 0.5 mM EDTA, 1 mM DTT, 4% glycerol, pH 8.0). The resuspended vesicles were then incubated for 1 h at room temperature, pelleted and resuspended a second time, and incubated for a second hour. The thoroughly stripped membranes were then pelleted a final time and resuspended in buffer B (50 mM HEPES, 0.5 mM EDTA, 2.5 mM $MgCl_2$, pH 8.0). After stripping, the presence of intact F_0 was verified by measuring the ATP hydrolysis activity bound to the membrane after addition of purified F_1. Recovery of activity was typically 95–100%. For the real-time stripping experiments unstripped vesicles were deposited initially, and stripping was carried out in situ using 1 M KSCN [21].

In some experiments, the hydrophilic portion of the b subunit was removed by trypsinization of the F_0 liposomes. The liposomes were incubated for up to 1 h with a trypsin to protein ratio of 1:25 (w/w). The reaction was stopped by dilution of the sample and centrifugation. The cleavage of the b subunit was monitored using SDS-PAGE by the disappearance of the 17 kDa band.

For experiments with c-subunit oligomers, the c subunit was isolated from the full ECF_1F_0 complex by diethyl ether extraction, either of the stripped F_0 liposomes or of unstripped F_1F_0 liposomes [22–24]. In the latter case, the absence of the other F_1F_0 subunits after extraction was verified by SDS/PAGE. After extraction, the diethyl ether phase containing lipids and c subunit was sonicated with buffer A, the ether slowly evaporated as described in Szoka and Papahadjopoulos [18], and the vesicle suspension filtered through polycarbonate membranes as described above.

2.2. Scanning force microscopy

To deposit the samples for SFM imaging, the reconstituted proteoliposome suspension was diluted with buffer B (50 mM HEPES-NaOH, 0.5 mM EDTA, 2.5 mM $MgCl_2$, pH 8.0) to 50 μg/ml lipids, a droplet of the diluted suspension was place on clean parafilm, and a freshly cleaved mica sheet floated on top. Excess liquid was absorbed with filter paper, while allowing the remaining suspension to spread on the mica surface. After about 20 min, the mica was rinsed thoroughly with buffer B, and the wet samples were inserted directly into the tapping mode fluid cell of a Nanoscope III SFM (Digital Instruments, Santa Barbara), filled with buffer B. The experiments on all F_1F_0-related systems were carried out using commercial silicon nitride triangular cantilevers with force constant approx. 0.3 N/m and resonance frequency 30–40 kHz (in air) or, on a few occasions, force constant 0.06 N/m and resonance frequency near 15 kHz (in air) [25]. In all cases the original pyramidal tips on these cantilevers were enhanced with 'e-beam' tips grown by electron-beam deposition in a scanning electron microscope [26,27]. Imaging was performed at tapping frequencies between about 8 and 40 kHz, depending on the response characteristics of individual cantilevers. The set-point voltage (tapping force) was set to the minimum value consistent with good tracking of the sample surface. At high set point values the sample was damaged, and at very low values the SFM feedback loop was not able to follow the surface. After acquisition, images were usually flattened using the Nanoscope software to remove background bands and slopes caused by laser mode switching and thermal drift. Enlargements of specific regions within larger images were created by bilinear interpolation. SFM images are intrinsically three dimensional in nature (maps of sample height vs. *xy* position), and can be displayed either as two-dimensional gray-scale maps (Fig. 1) or as three-dimensional surfaces (Fig. 3) without additional processing.

3. Results

3.1. SFM images of F_0

Three types of samples were imaged: unmodified ECF_0, trypsin-treated ECF_0 and reconstituted complexes containing only the c subunit. Fig. 1 is a tapping mode SFM image of ECF_0 in egg phosphatidylcholine (egg PC) membrane adsorbed to a mica substrate in buffer. Attempts to image the same samples in contact mode were usually not successful, due to increased shear force between the tip and the sample. The area shown is an enlarged region (825 nm square) from an image acquired at larger scan size (about 1.5 μm square). At scan sizes smaller than about 1 μm, damage increased to unacceptable levels. This is because as the scan size is reduced, individual protein particles receive an increasing number of tip-sample contacts in the course of collecting an image. The total 'exposure' thus increases with increasing magnification, much as in electron microscopy. The conditions reported represent the best compromise between maximum areal pixel density and minimum sample damage. Under optimum conditions, one or two images could be collected from a single sample area of about 1–2 μm before damage became severe. The image in Fig. 1 contains a number of uniformly sized particles which are absent in control samples without protein, and were therefore tentatively identified as ECF_0 complexes. Subsequent real-time stripping experiments confirmed this assignment (see below). The apparent diameter of the particles is in the range 15–22 nm, which is several times larger than the estimated diameter for F_0. Exaggeration of the lateral dimensions is a common feature of SFM images, caused by the relatively large size of the probe tip [11,28,29]. Assuming a typical tip end radius of 10 nm and the measured average height above the membrane of 1.5–2 nm, the estimated actual diameter is 6–7 nm, as expected for ECF_0. ECF_0 membranes were examined in many experiments in which the lipid-to-protein ratio was varied, and with many different probe tips. The quality of the images was quite variable but, in a few instances, a large number of the particles showed a characteristic ring and dimple, as can be seen in several particles in Fig. 1. Enlarged images of five of these particles (labeled a–e) are shown as insets at the bottom of Fig. 1. There is considerable variation, but the main qualitative features – the ring, dimple, and asymmetric mass – are clearly visible in all five, as well as in other particles within the field of view shown in Fig. 1.

3.2. Real-time stripping

In principle, ECF_0 or ECF_1F_0 membranes may deposit on the mica substrate either face up, with the cytoplasmic surface of F_0 accessible to the SFM tip, or face down, with the periplasmic surface exposed. To determine which face of the ECF_0 complex was visible, and to verify the identity of the particles shown in Fig. 1, a real-time stripping experiment was performed. Reconstituted ECF_1F_0 vesicles were deposited on mica and placed in the SFM fluid cell as before. Several initial images were taken and then the fluid cell was flushed with a stripping solution (1 M KSCN) to rapidly solubilize the F_1 sector, leaving the F_0 sector in the membrane. Before stripping, the images showed many high, structureless particles. After exposure to the stripping solution for a few minutes, the particle height decreased and the characteristic ring-and-dimple features of the F_0 sector appeared. A histogram of particle heights taken before and after stripping shows a large shift to lower values and a narrowing of the distribution after stripping (Fig. 2). The broad distribution of heights in Fig. 2A is consistent with some loss of F_1 even before stripping, or with a tendency for the SFM tip to push aside the relatively unstable F_1 sector during imaging. After stripping, the mean height of the particles changed from 6.9 ± 1.5 to 4.4 ± 1 nm,

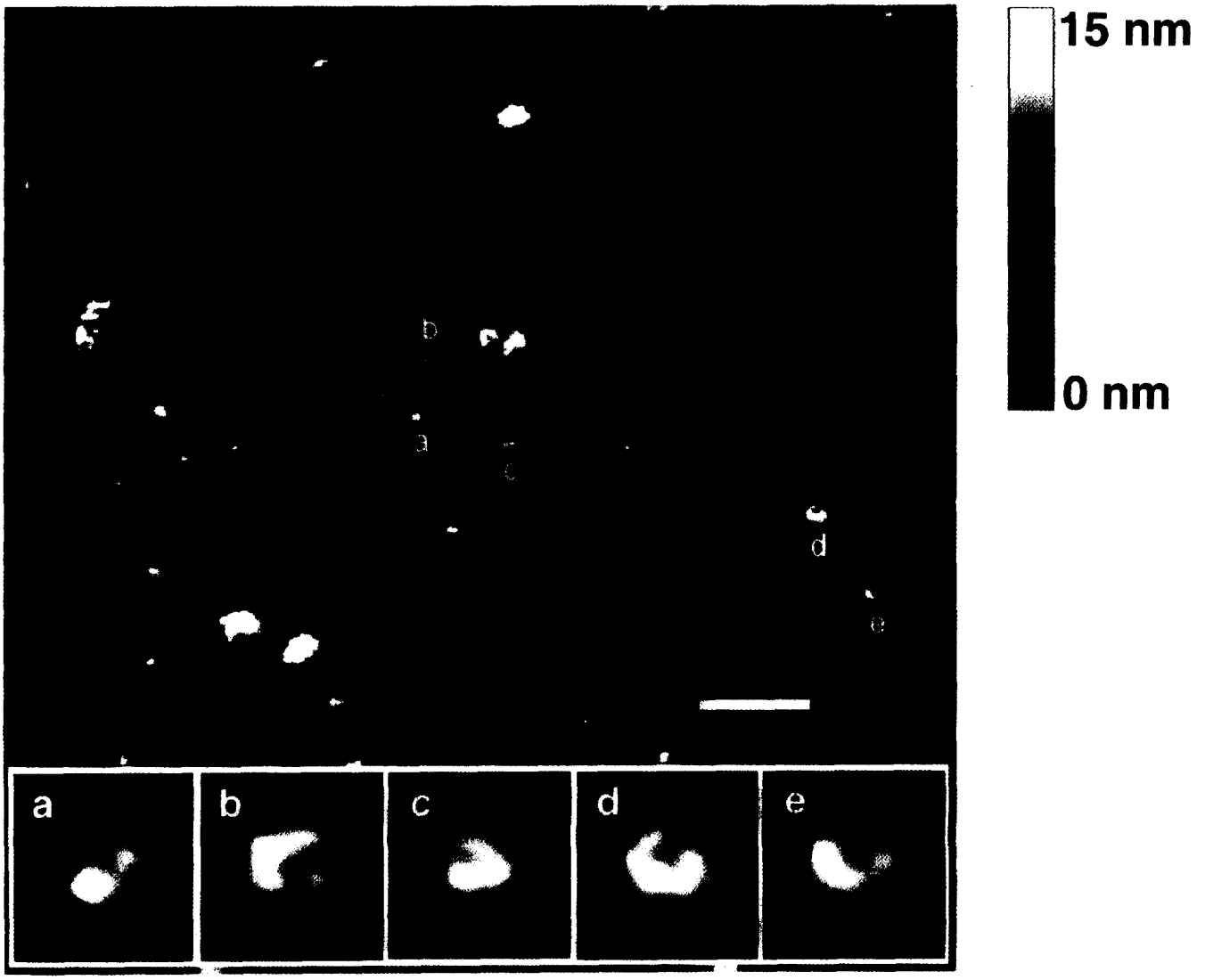

Fig. 1. SFM image of ECF_0 in egg phosphatidylcholine membrane. The area shown was enlarged by bilinear interpolation from an original image of 512×512 pixels collected at the 1.5 μm scale. Particles labeled a–e are shown in enlarged views (insets). Scale bar, 200 nm.

but a more meaningful comparison is between the largest significant values in the 'before' distribution, about 10 nm, and the peak of the 'after' distribution, about 3–3.5 nm. This is a change of almost 7 nm, consistent with the loss of the F_1 sector. The preferred orientation of the membranes on mica is therefore face up, with the cytoplasmic surfaces of F_0 and F_1F_0 exposed to view. The 'ring-and-dimple-with-lateral-mass' is clearly the F_0 sector.

3.3. SFM images of modified complexes

To help assign the ring and lateral mass to specific F_0 subunits, images of the complete F_0 complex were compared to images of two modified complexes: trypsin-treated ECF_0 and c-subunit oligomers. Trypsin is known to cleave preferentially the b subunit of ECF_0, so a change in the appearance of trypsin-treated ECF_0 should indicate the location of the b subunits. Likewise, the c subunit can be purified and reconstituted into membranes without the a and b subunits, where it forms an oligomeric complex. Comparison of these oligomers to intact ECF_0 should then allow the features associated with the c subunits to be identified.

Fig. 3 is a montage of images of single particles of either ECF_0 (left-hand column), trypsin-treated ECF_0 (middle column), or c-subunit oligomers (right-hand column). The particles are displayed as three-dimensional surfaces to better show changes in height of the asymmetric mass. Comparison of the first and second columns shows that after cleavage of the b subunit the lateral mass is shorter, but still present. Comparison of the first two columns with the third shows that the c-subunit oligomer has the ring-and-dimple appearance, but has no clear lateral mass. The most reasonable interpretation of these results is that the lateral mass contains the two b subunits and the ring and dimple features are associated with the 9–12 c subunits.

4. Discussion

Three main structural features of ECF_0 have been identified by the SFM: a ring with a central dimple and an asymmetric mass. Since trypsin cleavage of the b subunits reduces the size of the asymmetric mass, we conclude that the b subunits have a peripheral location, as in the model of Deckers-Hebestreit and Altendorf [9] (see also [30]), and are not centrally located as in the model of Cox et al. [10]. Since the ring and dimple

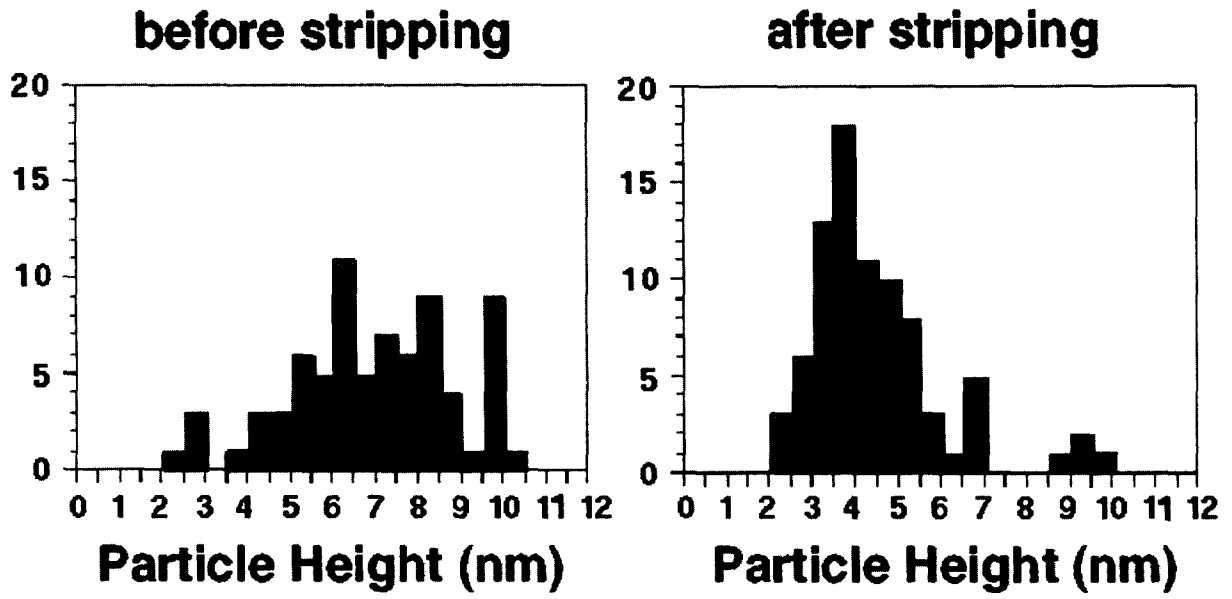

Fig. 2. Analysis of SFM images of membrane bound ECF_1F_0 complexes (a) before stripping the F_1 part, and (b) after stripping. Histograms are presented showing the distribution of heights before (a) and after (b) stripping. Before stripping, the distribution is broad with many high particles. After stripping, the distribution has a well-defined maximum near 3.5 nm, and shows few high particles.

are present in the c-oligomer complex, which contains no a or b subunits, we conclude that the c subunits form a ring structure, as suggested in several models for ECF_0. A number of proteins homologous to subunit c are known to form channels and pores [31]. The gap junction-like protein from *Nephrops norvegicus*, which has homology to both subunit c and also to

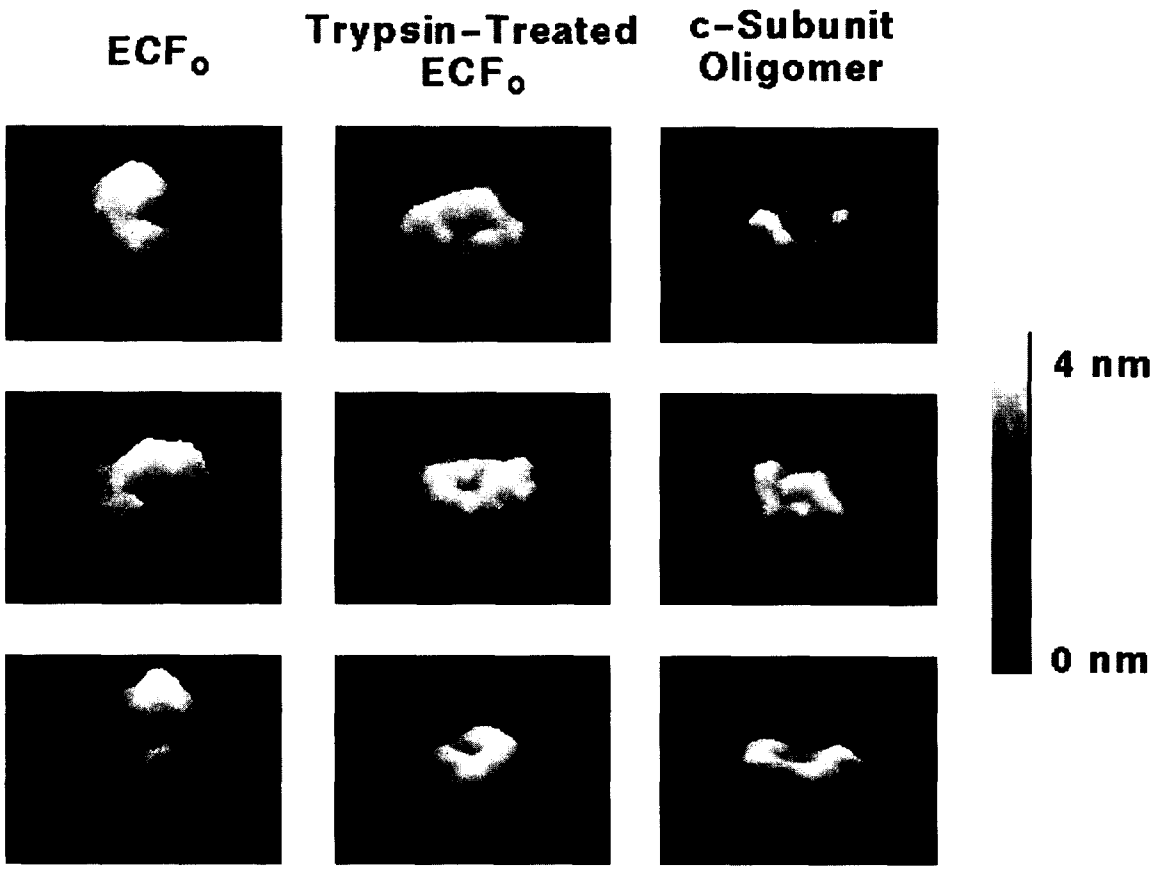

Fig. 3. Montage of nine single-particle images in three-dimensional projection: three ECF_0 particles (left-hand column), three trypsin-treated ECF_0 particles (middle column), and three c-subunit oligomers (right-hand column). Comparison across the columns shows that the lateral mass is reduced in height after trypsin treatment and is absent in the c-subunit oligomers. All images were interpolated to increase the number of pixels. The vertical scale has been stretched relative to the lateral scale to enhance the visibility of low features.

the c-subunit analog in the V-type ATPases, forms well-defined ring-like oligomers which can be crystallized into two dimensional arrays and analyzed by electron diffraction. Their structure is similar to the ring-and-dimple found here for the c oligomer. Thus, both the results presented here and the results of studies on related proteins are consistent with the idea that the c oligomer is a distinct, well-defined functional entity within the larger ECF_0 complex.

The a subunit was not clearly identified in the present study, and its location is still unknown: it could be in the asymmetric mass or in the center of the c-ring. Since the a subunit is quite accessible to lipid-soluble reagents [32], its most probable location is outside the ring in the asymmetric mass. We are now attempting to localize the a subunit by labeling experiments with monoclonal antibodies or with gold clusters. Longer term, we hope to obtain more detailed structural information on the ECF_0 complex. To do this, it will be important to explore systematically imaging conditions to minimize damage, and to apply image averaging techniques to the SFM data [33]. Preliminary calculations suggest that single-particle statistical methods can be applied to SFM images in much the same way as to electron microscope data [34].

From a methodological perspective, these results show that isolated membrane-bound complexes as small as ECF_0 (140–165 kDa, 6–7 nm diameter) can be imaged in physiological buffer using tapping mode SFM. The effective resolution is about 30 Å laterally and 2–5 Å vertically, and it has been possible to distinguish structural changes in related molecules. Earlier experiments on ECF_1F_0 using contact mode SFM were not successful, and the ability to use tapping mode in aqueous solution [25] has played a crucial role in our results. Finally, one of the most exciting aspects of SFM imaging is the ability to observe structural changes on single molecules in real-time or almost-real-time [11]. Several models for the ATP synthases suggest a physical rotation of the F_1 sector relative to F_0 [1,5,35], or rotation of the c oligomer relative to the a and b subunits [36]. The success of these initial experiments may help to pave the way for future experiments in which such models can be tested by direct imaging.

Acknowledgements: The authors would like to thank Kathy Chicas-Cruz for help with protein preparation. This work was partially supported by National Institutes of Health Grants GM 32543 (C.J.B.) and HL 24526 (R.A.C.) and by National Science Foundation Grants NBC 9118482 and BIR 9318945 (C.J.B.).

References

[1] Capaldi, R.A., Aggeler, R., Turina, P. and Wilkens, S. (1994) Trends Biochem. Sci. 19, 284–289.
[2] Senior, A.E. (1990) Annu. Rev. Biophys. Biophys. Chem. 19, 17–41.
[3] Fillingame, R.H. (1990) in: The Bacteria: A Treatise on Structure and Function, vol. XII (Krulwich, T.A. ed.) pp. 345–391, New York Academy Press, New York.
[4] Lücken, U., Gogol, E.P. and Capaldi, R.A. (1990) Biochemistry 29, 5339–5343.
[5] Abrahams, J.P., Leslie, A.G.W., Lutter, R. and Walker, J.E. (1994) Nature 370, 621–628.
[6] Wilkens, S., Dahlquist, F.W., McIntosh, L.P., Donaldson, L.W. and Capaldi, R.A. (1993) Nat. Struct. Biol. 2, 961–967.
[7] Berzborn, R.J., Klein-Hitpass, L., Otto, J., Schunemann, S., Owarah-Nkruma, R. and Meyer, H.E. (1990) Z. Naturforsch. 45c, 772–784.
[8] Walker, J.E., Lutter, R., Dupuis, A. and Runswick, M.J. (1991) Biochemistry 30, 5369–5378.
[9] Deckers-Hebestreit, G. and Altendorf, K. (1992) J. Exp. Biol. 172, 451–460.
[10] Cox, G.B, Fimmel, A.L, Gibson, F. and Hatch, L. (1986) Biochim, Biophys. Acta 849, 62–69.
[11] Bustamante, C. and Keller, D. (1995) Phys. Today 48, 32–38.
[12] Karrasch, S., Hegerl, R., Hoh, J.H., Baumeister, W. and Engel A. (1994) Proc. Natl. Acad. Sci USA 91, 836–838.
[13] Yang, J., Tamm, L.K., Tillack, T.W. and Shao, Z. (1993) J. Mol. Biol. 229, 286–290.
[14] Pante, N. and Aebi, U. (1993) J. Cell Biol. 122, 977–984.
[15] Mou, J., Yang, J. and Shao, Z. (1995) J. Mol. Biol. 248, 507–512.
[16] Foster, D.L, Mosher, M.E. and Fillingame, R.H. (1980) J. Biol. Chem. 255, 12037–12041.
[17] Aggeler, R., Zhang, Y. and Capaldi, R.A. (1987) Biochemistry 26, 7107–1113.
[18] Szoka, F., Jr. and Papahadjopoulos, D (1978) Proc. Natl. Acad Sci. USA 75, 4194–4198.
[19] Richard, P, Rigaud, J.L. and Graber, P (1990) Eur. J. Biochem. 193, 921–925.
[20] Lötscher, H-R., DeJong, C. and Capaldi, R.A. (1984) Biochemistry 23, 4128–4134.
[21] Perlin, D.S., Cox, D.N. and Senior, A.E. (1983) J. Biol. Chem. 258, 9793–9800.
[22] Cattell, K.J., Lindop, C.R., Knight, I.G. and Beechey, R.B. (1971) Biochem. J. 125, 169–177.
[23] Sierra, M.F. and Tzagaloff, A. (1973) Proc. Natl. Acad. Sci. 70, 3155–3159.
[24] Fillingame, R.H. (1976) J. Biol. Chem. 251, 6630–6637.
[25] Hansma, P., Cleveland, J.P., Radmacher, M., Walters, D.A., Hillner, P.E., Bezanilla, M., Fritz, M., Vie, D. and Hansma, H.G. (1994) Appl. Phys. Lett. 64, 1738–1740.
[26] Keller, D. and Chou, C.C. (1992) Surface Sci. 268, 333–339.
[27] Keller, D., Deputy, D., Alduino, A. and Luo, K. (1992) Ultramicroscopy 42-44, 1481–1486.
[28] Keller, D. and Franke, F. (1993) Surface Sci. 294, 409–419.
[29] Keller, D. (1991) Surface Sci. 253, 353.
[30] Schneider, E. and Altendorf, K. (1987) Microbiol. Rev. 51, 477–497.
[31] Holzenburg, A., Jones, P.C., Franklin, T., Pali, T., Heimburg, T., Marsh, D., Findlay, J.B. and Finbow, M.E. (1993) Eur. J. Biochem. 213, 21–30.
[32] Steffens, K., Hoppe, J. and Altendorf, K. (1988) Eur. J. Biochem. 170, 627–630.
[33] Van Heel, M. and Frank, J. (1981) Ultramicroscopy 6, 187–194.
[34] Wilkens, S. and Capaldi, R.A. (1994) Biol. Chem. Hoppe-Seyler 375, 43–51.
[35] Boyer, P.D. (1993) Biochim. Biophys. Acta 1140, 215–250.
[36] Vik, S.B. and Antonio, B.J. (1994) J. Biol. Chem. 269, 30364–30369.